STRUCTURE AND CHEMICAL DURABILITY OF LEAD CRYSTAL GLASS

Frederic Angeli, Patrick Jollivet, Thibault Charpentier, Maxime Fournier, S. Gin

HAL Id: cea-02388823

https://cea.hal.science/cea-02388823

Submitted on 2 Dec 2019

STRUCTURE AND CHEMICAL DURABILITY OF LEAD CRYSTAL GLASS

Frédéric Angeli[a], Patrick Jollivet[a], Thibault Charpentier[b], Maxime Fournier[a], Stéphane Gin[a]

[a]CEA, DEN, DTCD, SECM, F-30207 Bagnols-sur-Cèze, France

[b]NIMBE, CEA, CNRS, Université Paris-Saclay CEA Saclay 91191 Gif-sur-Yvette, France

ABSTRACT

Silicate glasses containing lead, also called lead crystal glasses, are commonly used as food product containers, in particular for alcoholic beverages. Lead's health hazards require major attention, which can first be investigated through the understanding of Pb release mechanisms in solution. The behavior of a commercial glass containing 10 mol% of PbO (28 wt%) was studied in a reference solution of 4% acetic acid at 22, 40 and 70°C at early and advanced stages of reaction. For the first time, high-resolution ^{17}O solid-state NMR was used to probe Pb in the pristine and altered crystal glass. Inserted into the vitreous structure between the network formers as Si-O-Pb bonds, Pb does not form Pb-O-Pb clusters which are expected to be more easily leached. A part of K is located near Pb, forming Si-O-(Pb,K) mixing areas near the non-bridging oxygens. Pb is always released into the solution following a diffusion controlled process over various periods of time, at a rate between one and two orders of magnitude lower than the alkalis (K and Na). The preferential release of alkalis is followed by an *in situ* repolymerization of the silicate network. Pb is only depleted in the outermost part of the alteration layer. In the remaining part, it stays mainly surrounded by Si in a stable structural configuration similar to that of the pristine glass.

32

INTRODUCTION

33

34

35   For thousands of years, lead has been used in the preparation of silicate glasses, in particular

36 because it enables the temperature range of the glass-forming ability to be extended. It was widely

37 used in various archeological artifacts, such as enamels and glazes [1], but also in applications for

38 optics, electronics [2] or even in protection against irradiation [3]. Since the 17th century, lead oxide has

39 been added to alkali silicate to form a material called lead crystal, giving a high clarity and a

40 characteristic sonority. Lead crystal has been regulated since 1969 in order to guarantee the quality of

41 the material, based on density, refraction index and lead content criteria. Lead oxide must be at least

42 24 wt% to be designated as crystal.

43   Exposure to Pb is hazardous for the environment and for human health when it accumulates in

44 the organism [4, 5]. It is therefore of primary importance to understand the behavior of this element in

45 manufactured articles throughout their conditions of use, particularly if they contain liquids intended for

46 human consumption.

47   Numerous empirical studies have been carried out to examine the Pb leaching from glass or

48 from glass ceramic in reactive environments, particularly in contact with different actual beverages or

49 simple synthetic solutions such as acetic acid or nitric acid [6-20]. In commercial lead crystal glasses, it

50 has generally been observed that the release of alkalis and Pb ions exhibited a square root time

51 dependence through a diffusion process [11, 15, 17, 18]. Their leaching kinetics usually increase with the

52 temperature and with the acetic acid concentration [17]. During successive contacts, a decrease in the

53 release of Pb has been observed with each additional solution contact [16]. However, there is a lack of

54 mechanistic understanding able to account for and predict the Pb behavior, in relation with its

55 structural evolution during leaching.

56   The structural arrangements coming from the incorporation of Pb into an alkali silicate network

57 can significantly modify glass macroscopic properties, in particular its chemical durability [10]. For a low

58 content, typically under 40 mol% of PbO, a major part of Pb may be assimilated to a modifier cation [21],

59 thus resembling an alkaline-earth type cation, forming ionic bonds with non-bridging oxygens (NBOs)

60 [22]. When a large amount of Pb is added to reach an orthosilicate composition (Pb/Si = 2), oxygens are

61 then linked to the metallic cations to form metal-bridging oxygen bonds Pb-O-Pb [23]. Pb is then

62 associated in trigonal pyramids connected by their edges to form interlinked Pb_2O_4 units [24]. In this

63 case, Pb mainly takes a network former configuration, forming more covalent bonds with the oxygens

64 [21, 25, 26]. For contents greater than ~60 mol% of PbO, Pb forms its own vitreous network [27]. Pb has the

65 special feature of having ability to form a glass in a very wide range of concentration [28], up to more

66 than 80 mol% of PbO for a rapidly-quenched glass [23, 27]. When Pb acts as a network former cation,

67 unlike most network formers, it does not provide to the glass a greater chemical durability: Pb clusters

68 form extended lead-rich domains which are rapidly leached. There are percolation pathways between

69 these domains, and the Pb release into solution strongly increases [10]. Generally, whatever the solution

70 pH, the release of Pb seems to decrease when its content is lower [10, 19, 29].

71 The mechanisms of aqueous alteration of lead crystal glasses compared to their structural

72 evolution during leaching had not been approached prior to this study. In order to give new insights

73 into the understanding of Pb leaching of industrial glasses, a structural approach for the glass as well

74 as its alteration layer is applied, together with the evolution of the elemental alteration profiles.

75 Combined with the solution analyses under various experimental conditions, it enables the

76 mechanisms involved to be better defined.

77 This work is focused on a commercial lead crystal glass containing 10 mol% of PbO (28 wt%).

78 Complementary experiments, which enabled various kinetics regimes to be reached, are conducted to

79 simulate the short and long term behavior of the crystal glass. Hydrolysis mechanisms were

80 investigated using dynamic experiments with high flow rate whereas interdiffusion mechanisms were

81 highlighted from static experiments using saturated solutions with respect to amorphous silica (ion-

82 exchange processes are not affected by solution saturation). The experiments were carried out in 4%

83 (*v/v*) acetic acid solution, which is commonly used as a standard reference solution [13, 17, 30]. The local

84 structure of pristine and altered materials was characterized by high-resolution solid-state Nuclear

85 Magnetic Resonance (NMR) of silicon-29 and oxygen-17. Elemental depth profiling were monitored by

86 Time-of-Flight Secondary Ion Mass Spectrometry (ToF-SIMS).

87

88 **EXPERIMENTAL**

89 **Materials**.

90 Two glasses were used for this study, the first being a commercial glass with the molar

91 composition $77.1SiO_2 - 0.8Na_2O - 11.3K_2O - 10.6PbO - 0.2Sb_2O_3$. A second glass was synthetized

92 to be enriched in oxygen-17 (without Sb addition). 200 mg of glass was prepared by sol-gel from a

93 mixture of alkoxides hydrolyzed by 90% enriched water in ^{17}O [31]. After reaction, this mixture was

94 maintained at 1270 °C for 30 minutes under argon atmosphere in a Pt/Au crucible. ICP-OES analysis

95 after acidic dissolution ($HCl+HNO_3+HF$) gave the molar composition: $80.7SiO_2 - 0.7Na_2O - 10.8K_2O -$

96 7.9PbO.

97

98 **NMR.**

99 ^{29}Si MAS NMR data were collected on a Bruker 300WB Avance I spectrometer operating at a

100 magnetic field of 7.02 T. ($I = 1/2$, Larmor frequency $\nu_0 = 59.4$ MHz). A Bruker 4 mm (outer diameter of

101 the rotor) CPMAS Probe was used at a spinning frequency of 10 kHz. Silicon spectra were acquired

102 using the CPMG sequence [32], by typically accumulating 32 echoes with an echo delay of 4 ms
103 between consecutive 180° pulses. The echoes were th en summed up and Fourier transformed to
104 obtain the spectra. A 20 s recycling time was used; checks were carried out that no spectral
105 deformation was observed for longer recycling delays (up to 1200 s). The spectra were referenced to
106 an external tetrakis(trimethylsilyl)silane (TKS) sample, for which the highest intensity peak was
107 situated at –9.9 ppm from that of TMS.

108   ^{17}O MAS NMR data were collected on a Bruker 500WB Avance II spectrometer operating at a
109 magnetic field of 11.72 T (I = 5/2, Larmor frequency ν_0 = 67.67 MHz,). A Bruker 4 mm CPMAS probe
110 was used at a spinning frequency of 12.5 kHz. MAS NMR spectra were acquired using a rotor
111 synchronized Hahn echo pulse sequence to minimize the baseline distortion, with soft 90° and 180°
112 pulses (selective on the central transition, RF field 25 kHz), an echo delay of one rotation period and a
113 recycle delay of 1 s (no change in lineshape was observed for longer delay). The MQMAS spectra
114 were acquired with 64 t_1 rotor-synchronized increments (of one rotation period) in the first dimension
115 and a 1 s repetition time (4500 FIDs per t_1 value were collected). The Z-filter pulse sequence [33] was
116 used with first and second pulse durations of 5 μs and 2 μs, respectively (RF field 60 kHz), and a third
117 90° soft pulse, selective on the central transition , of 3.5 μs (RF field 25 kHz) [34].

118   All data were processed and fitted using an in-house written software [35].

119

120 **ToF-SIMS**.

121   Depth profiles were analyzed by ToF-SIMS IONTOF® TOF 5 using O_2^+ sputtering beams
122 analyzing a surface area of 60 x 60 μm^2. Oxygen beam was tuned at 2 kV, 500 nA. Elemental profiles
123 were normalized to that of Si to avoid matrix effects.

124

125 **Leaching experiments.**

126   After crushing and sieving, the selected size fractions (20-40 and 63-125 μm) were washed by
127 decantation in acetone and absolute ethanol to remove fine particles, according to Stokes' law. Then
128 the specific surface areas of the glass powders were measured by krypton physical adsorption on the
129 sample surface with the BET method on a Micromeritics ASAP 2020.

130   Forward dissolution rate r_0 was measured using a single-pass flow-through test (SPFT) at 22,
131 40 and 70 °C. About 100 mg of glass powder (63-125 μm particle size fraction) were placed into a
132 column made of PTFE tube, through which 4% (*v/v*) acetic acid was passed at a flow rate between 0.2
133 and 0.6 mL/min to avoid any feedback effect on the rate by glass constituent elements released into
134 solution. The temperature of the leaching solution was monitored continuously at the reactor inlet and
135 a maximum variation of ± 1 °C was allowed. The leachate was regularly sampl ed and the Si
136 concentration was determined photometrically with a Merck Spectroquant test and a Cary Varian UV-

4

137 visible spectrophotometer with a method analogous to ASTM D859-10. Taking into account the errors

138 on the glass surface area and the Si concentration, the uncertainty on r_0 was about 10%. The

139 normalized mass losses, NL_i, (g.m^{-2}) were calculated with the equation (1):

140

$$NL_i(t) = \sum_{j=1}^{j=n} \frac{1}{x_i \times SSA \times m} \left[\frac{(C(i)_j + C(i)_{j+1})}{2} \times Q \times (t_{j+1} - t_j) \right] \qquad (1)$$

141 with j the sampling, $C(i)_j$ the concentration of the element in the jth sampling, Q the solution flow rate,

142 SSA the specific surface area of powder sample, m the mass of glass, x_i the weight fraction of element

143 i in the glass, and $t_{j+1} - t_j$ the time between two samplings.

144
145   Alteration in static conditions was measured in perfluoroalkoxy reactors (PFA) at 22, 40 and

146 70 °C in 4% (v/v) acetic acid solution. The mass of glass powder (20-40 μm and 63-125 μm particle

147 size fractions) was adjusted to have the desired glass-surface-area-to-solution-volume ratios (SA/V).

148 The solutions were ultrafiltered (cutoff 10 kDa) and analyzed by ICP-OES.

149

$$NL(i)_t = NL(i)_{t-1} + \frac{(C(i)_t - C(i)_{t-1}) \times V_t}{SSA \times m \times x_i} \qquad (2)$$

150 with $C(i)_t$ the concentration of the element i in solution at time t, and V_t the volume of solution

151 sampling at time t.

152 The equivalent thickness of altered glass is given by:

153

$$ETh(i) = \frac{NL(i)}{\rho} \qquad (3)$$

154 ρ is the glass density (3.028.10^6 kg.m^{-3}). The uncertainties for $ETh(i)$ and the alteration rate

155 $r = \mathrm{d}ETh(i)/\mathrm{d}t$ are of 10% and 30%, respectively.

156

157 **RESULTS AND DISCUSSION**

158 **Glass structure**

159 **^{29}Si MAS NMR.**

160   Two contributions were observed at –94 ppm and –106 ppm on the ^{29}Si MAS NMR spectra for

161 pristine glass (Figure 1a), which correspond respectively to the Q^3 and Q^4 entities, in agreement with

162 the data obtained on lead silica binary glasses [36, 37]. The simulation of the ^{29}Si spectra gave a

163 proportion of 59% of Q^3 and 41% of Q^4 units (see supplementary information, Figure S1). The

5

164 resulting number of NBOs is then 25.7%. The calculation of the NBOs based on the glass

165 composition, considering that two NBOs are formed from Na_2O, K_2O and PbO (without postulating free

166 oxygen atoms) leads to a value of 25.6%, very close to the experimental value.

167

168 **^{17}O MAS NMR.**

169 The [17]O MAS spectrum of the pristine glass (Figure 1b) enables three contributions to be

170 resolved. A wide line at the −20 to 50 ppm range with a characteristic second-order quadrupolar

171 lineshape corresponds to the bridging oxygens Si-O-Si. Two narrower featureless peaks centered on

172 70 and 110 ppm are related to the NBOs and may be attributed to Si-O-K and Si-O-(Pb,K),

173 respectively (the latter corresponds to regions where Pb and K are mixed together but without forming

174 Pb-O-Pb bonds). This attribution will be discussed hereafter from the MQMAS data.

175

176 **^{17}O MQMAS NMR.**

177 The three contributions related to Si, K and Pb are clearly separated on the experimental and

178 simulated [17]O MQMAS spectra shown in Figure 2a. The simulated spectra, generated using a 3D

179 distribution of the NMR parameters (taking into account the correlation effects between these

180 parameters [35]), show very good agreement with the experimental spectra (Figure 2a). Figure 2b shows

181 the two-dimensional projection of the distribution of the NMR parameters, the isotropic chemical shift

182 (δ_{iso}) and the quadrupolar coupling constant (C_Q) extracted from the MQMAS spectra. Lee and Kim [38]

183 recently reported the structural evolution of binary lead silicate glasses from ^{17}O MQMAS NMR for

184 high PbO contents close to the orthosilicate composition ranging from 60 mol% to 71 mol%. They

185 clearly pointed out the presence Pb-O-Pb bonds which increased with Pb content at the expense of Si-

186 O-Si bonds. They represented Pb and Si mixing sites in the form $^{[n]}Pb-^{[m]}O-^{[4]}Si$, where $n = 3,4$ and

187 $m = 2,3,4$. Under these conditions, the same oxygen atom could be involved in both Pb-O-Si and Pb-

188 O-Pb bonds. The absence of Pb-O-Pb contribution (within the NMR detection limit) in our crystal glass

189 suggests that Pb structural configuration may be fairly close to that of an alkaline-earth type network

190 modifier.

191 Furthermore, the nature of the alkali cation at the origin of the NBO formation may modify the

192 position of the [17]O line; a sodium disilicate decreases the NBO δ_{iso} by about 40 ppm compared to a

193 potassium disilicate [39]. The position of the NBO site at around 75 ppm can be attributed here to Si-O-

194 K, Si-O-Na being expected at around 40 ppm [35]. Given the low Na content in the glass (below one

195 percent) and the sensitivity of the MQMAS experiment, it remains challenging to observe Si-O-Na

196 contribution on the [17]O MQMAS spectra.

197 A previous work carried out on a binary sodium silicate glass with a 77 mol% SiO_2 content

198 close to that studied here reported ^{17}O NMR parameters for the Si-O-Si site similar to those obtained

199   for our lead glass [35]. Under these conditions, the addition of Pb to the glass does not seem to have a

200   major effect on the Si-O-Si site geometry, either for the angular distributions (which influence the

201   quadrupolar parameters [40-42]) or the Si-O bond distances (which influence the isotropic chemical shift

202   [43, 44]). In the binary lead silicate glasses studied by Lee and Kim [38], the Si-O-Pb δ_{iso} was located

203   around 151 ppm and it slightly increased with Pb content. For our glass composition, the contribution

204   related to Pb is close to 119 ppm (see Table 1). The quantification of the three oxygen contributions

205   enables the origin of this difference to be discussed.

206   By first assuming that the three ^{17}O sites revealed by the NMR spectra can be attributed to the

207   contributions of Si-O-Si, Si-O-Pb and Si-O-K, Table 1 compares their proportions calculated from the

208   crystal glass chemical composition and those obtained from the NMR data. It clearly appears that the

209   quantity of Si-O-Pb (14%) is considerably greater than expected from the composition (8.7%), unlike

210   for Si-O-K where the quantity is lower (8% experimentally instead of the expected 12.7%). This

211   observation indicates that Si-O-Pb contribution does not only contain Pb and Si cations, but rather a

212   mixing of Pb and K, noted Si-O-(Pb,K), as had been previously observed for other types of cations

213   having fairly close ionic radii [45, 46]. Under these conditions, Si-O-(Pb,K) site would consist of 38% of K

214   and 62% of Pb. This effect thus explains the lower [17]O δ_{iso} of the Si-O-Pb site in the glasses studied

215   here compared to the binary glasses [38]; Si-O-(Pb,K) site at 119 ppm is situated between Si-O-K at 75

216   ppm and Si-O-Pb at 151 ppm. Finally, it should be noted that the wider distribution of [17]O δ_{iso} for Si-O-

217   (Pb,K) is probably the result of a greater structural and/or chemical disorder for this mixing site.

218   It is worth noting that by taking into account the difference in chemical shift between Si-O-Pb

219   at 151 ppm and Si-O-K at 75 ppm, weighting of the value obtained for Si-O-(Pb,K) at 119 ppm would

220   give a K quantity of 42%, very close to the value directly deduced from the quantification of the

221   MQMAS spectrum (38%). It would therefore appear that [17]O δ_{iso} of Si-O-(Pb,K) could provide

222   information regarding the proportion of K mixing with Pb in the NBO environment.

223

224   **GLASS LEACHING.**

225   For the first set of experiments, the most favorable conditions for accessing silicate network

226   hydrolysis mechanisms were chosen, based on a high renewal rate of a 4% (*v/v*) acetic acid solution.

227   Figures 3(a,b,c) show the equivalent alteration thicknesses of Na, K, Pb and Si at 22, 40 and 70 ℃

228   calculated from their normalized mass losses (Eq. (3)). The leaching of Sb (not shown) is very close to

229   the Si. An activation energy for hydrolysis mechanisms in the forward dissolution rate regime, based

230   on an Arrhenius law, is given from the Si release (Figure 3d). The linearity between the three

231   temperatures shows the good agreement of the data, resulting in an activation energy of 38.7 ± 1.7

232   kJ.mol^{-1}. Within the temperature range studied (22-70℃), the release of Si leading to the hydrolysis of

233   the silicate network would thus seem to be controlled by the same mechanisms. It should be noted

234 that the dissolution was significantly non-congruent; while the release of Pb and Sb were fairly close to
235 the Si network former, K and Na were released much more rapidly. It is tricky to calculate unique
236 activation energy for Pb, K and Na as the non-linearity observed between the three temperatures
237 strongly suggest that the leaching of these elements could not only resulted from network hydrolysis
238 but also interdiffusion. At low temperature, the interdiffusion mechanism may probably favored
239 whereas at higher temperature hydrolysis may be prevalent.

240 For the second set of experiments, a solution initially saturated with respect to amorphous
241 silica [47] was used in order to specifically focus on the interdiffusion mechanisms. It has recently been
242 showed that there was no hydrolysis of Si under these conditions [47]. Figure 4(a,b,c) compares the
243 normalized mass losses for K and Pb at 22, 40 and 70 °C as a function of the square root of time. The
244 very low concentration of Na in the glass (0.2 mol%) made its measuring in solution only possible at
245 70°C. It was then observed that it behaved like K. Analogous behavior of Na and K is therefore
246 probable at lower temperatures.

247 The resulting linear behavior suggests that the different cations are released in solution by a
248 diffusive mechanism. The leaching of Pb was much lower than K. The Pb behavior thus seems to be
249 assimilated with multivalent elements, like the alkaline earths or the rare earth elements, which are
250 leached much more slowly than the alkalis [46]. Fick's second law was used to derive the apparent
251 diffusion coefficients at the interface between the glass and the solution by fitting the curves in Figures
252 4(a,b,c). The concentration in solution is then given by [48]:

$$C(i) = 2 \frac{SSA \times m}{V} x_i \left(\frac{D_i \times t}{\pi} \right)^{\frac{1}{2}} \qquad (4)$$

253 where $C(i)$ is the concentration of element i (i = K or Pb) in solution, x_i is the concentration of Pb or K
254 in the glass, V the volume of the solution and D_i the diffusion coefficient for Pb or K.

255

256 Figure 4d shows the evolution of the diffusion coefficients as a function of the temperature for
257 Pb and K. The resulting activation energies highlight a temperature dependence which is much lower
258 for Pb than for K, with values of 37.2 ± 6.5 kJ.mol^{-1} and 72.2 ± 7.6 KJ.mol^{-1}, respectively. At 22 °C, a
259 low diffusion coefficient of $(3.1 \pm 0.6).10^{-22}$ m^2.s^{-1} is determined for Pb. Depending on the temperature,
260 Pb release into solution is between one and two orders of magnitude slower than the alkalis.

261 For higher Pb contents, from 25 to 70 mol%, diffusion coefficients of more than four orders of
262 magnitude higher were obtained in glasses altered in 0.1 N or 0.5 N HNO$_3$ solutions [8, 10]. A percolation
263 mechanism through the plumbate sub-network was observed. Binary lead silicate glasses with PbO
264 starting from an approximately 33 mol% content, had a diffusion coefficient increasing by about one
265 order of magnitude when PbO content increased by 5% [10]. One single composition was studied at a

266 lower Pb content (25%) below the percolation threshold; it showed less pronounced diffusion

267 coefficient variations, of about 10^{-17} $m^2.s^{-1}$ suggesting a plateau. If this latter value is not taken into

268 account, so if the data located within the percolation regime are extrapolated from our glass

269 composition containing 10 mol% of PbO, a similar value (10^{-22} $m^2.s^{-1}$) compared to that found in our

270 study (10^{-21} $m^2.s^{-1}$) is obtained. This value is far away from the plateau which was observed at

271 approximately 10^{-17} $m^2.s^{-1}$ for 25 mol% of PbO (see supplementary information, Figure S2). Then, the

272 sharp drop in the diffusion coefficient could be due to a second percolation threshold, which would

273 explain the high difference between 10 and 25 mol% of PbO. The formation of Pb-O-Pb bonds with

274 the increase in the Pb concentration, even if they do not yet constituted a plumbate sub-network, could

275 lead to this first percolation threshold beyond which an increase in Pb release kinetics would occur.

276 Finally, in order to reach more advanced reaction progress, a third set of experiments were

277 carried out in static conditions at different *SA/V* ratios, varying from 10 m^{-1} to 10000 m^{-1}. These long

278 term experiments were conducted at 22 °C in 4% acetic acid solution, without Si in the initial solution,

279 for one year of leaching. Although there were four orders of magnitude between the surface ratios,

280 Figure 5 reports small variations in the leaching of Pb and K, showing that their releases remain

281 controlled by interdiffusion at 22 °C. As expected from our previous experiments, Pb leaching is much

282 lower than K. The calculation of the retention factor for Pb compared to K ($RF_{r(Pb)}=1-ETh(Pb)/ETh(K)$)

283 gave similar values, with an average retention of 77% of Pb in the alteration layer. It may be noted that

284 Pb concentrations in solution always remain much lower (by at least three orders of magnitude) than

285 the solubility of lead acetate [49]. This confirms that the release of Pb is not controlled by its solubility

286 limit, but rather by diffusion mechanisms.

287

288 **ALTERATION LAYER CHARACTERIZATION**

289 **ToF-SIMS.**

290 Figure 6 displays the elemental profiles obtained by ToF-SIMS on the glass altered at 70 °C in

291 an acetic acid solution saturated with respect to amorphous silica after 1, 7 and 53 days. The progress

292 of the alteration front on the glass surface is clearly visible over time. At the interface between the

293 pristine glass and the alteration layer, the hydration front can be seen progressing, with a greater

294 penetration of hydrogen compared to the alkalis depletion. The profiles for Na and K are very similar,

295 in agreement with the concentrations measured in solution (Figure 4c). Pb was clearly released to a

296 lesser extent than the alkalis, and is only depleted on a thin external surface of the alteration layer.

297 After 53 days, the depth of Pb depletion was fifteen times less than the total thickness of the alteration

298 layer. The equivalent thicknesses for the different elements are in quite good agreement with the

299 depths obtained from the ToF-SIMS profiles. The small differences which remained between the two

300 methods could be explained because (i) calculation of *ETh* using the *SSA* of glass powder measured

9

301   by BET underestimates *ETh* [50] (ii) a part of K (~20-30%) is retained in the alteration layer and

302   therefore not released in solution and (iii) it may exist variations in the abrasion rate of ToF-SIMS

303   between the alteration layer external surface and the pristine glass, because of potentially different

304   densities.

305   The elemental profiles obtained after one year of alteration at various SA/V ratios at 22 ℃

306   were very similar than the profiles obtained at 70 ℃ for shorter periods. In particular, the three areas

307   remain still observed: the hydration front, the alkalis depletion and the Pb-depleted external surface

308   which is still maintained for long term experiments (see supplementary information, Figure S3).

309

310   **MAS NMR.**

311   Small glass powders of a few microns were entirely altered under static conditions at 70℃ in a

312   4% acetic acid solution containing oxygen-17 enriched water, in order to specifically probe the

313   alteration layer by ^{17}O NMR. An experiment in oxygen-16 carried out in parallel and under the same

314   *SA/V* ratio conditions (but with a greater volume of solution), enabled the concentrations of elements in

315   solution to be measured. This allowed the experiment to be stopped when all the glass had been

316   altered, based on the release of Na in solution, and to estimate the alteration layer molar composition

317   deduced from the solution analysis: $88.7SiO_2 – 2.5K_2O – 7.9PbO – 1.0Sb_2O_3$.

318   Figure 1a compares the ^{29}Si MAS spectra for pristine glass and for glass altered in oxygen-17.

319   An obvious reorganization within the alteration layer through a silicate network polymerization is

320   clearly highlighted. Centered on the Q^2-Q^3 species in the pristine glass, a majority of the Si forms Q^4

321   units in the alteration layer. Quantification of the NBOs was carried out based on the ^{17}O NMR data of

322   Figure 1b (reported in Table 1). The ^{17}O MAS spectrum clearly confirms that most of K had been

323   released in solution whereas a significant part of Pb remained in the alteration layer. The line

324   corresponding to the Si-O-(Pb,K) contribution, shifted towards the higher chemical shifts, becomes

325   closer to the Si-O-Pb contribution observed in binary lead silicate glasses [38], indicating a lower level of

326   mixing between Pb and K. This shows that in the Si-O-(Pb,K) site, K is preferentially extracted

327   compared to Pb.

328   Simulation of the ^{17}O MAS spectrum for altered glass was used to estimate the composition of

329   the alteration layer from the various contributions. The following molar proportions were obtained:

330     $93SiO_2 – 1K_2O – 6PbO$ (there was no Sb in this glass), in quite good agreement with the mass

331   balance found from the solution analysis ($88.7SiO_2 – 2.5K_2O – 7.9PbO – 1.0Sb_2O_3$). It should however

332   be noted that the NMR indicates a higher SiO_2 content (93% instead of 89%). This is related to the

333   presence of Si-OH sites which overlay the Si-O-Si contribution on the spectrum [51]. These sites were

334   revealed from 2D heteronuclear correlations maps ($^1H{\rightarrow}^{17}O$ HETCOR) (see supplementary

335   information, Figure S4a). The NMR parameters considered for this site (Table 1) come from the work

336 of Brunet et al. [51]. Simulation of the ^{17}O MAS spectrum gave 4% of Si-OH sites (see supplementary

337 information, Figure S4b). The total number of NBOs of 11% is quite comparable to the number of

338 NBOs deduced from the alteration layer composition (10.9%). The repolymerization led to a decrease

339 in the NBOs, dropping from 22% in the glass to 11% in the alteration layer (Table 1). A significant

340 decrease can be noted for the widths of the NMR parameters distribution for the Si-O-Si site (related

341 to higher Si-O-Si mean bond angles), as well as an increase in the quadrupolar coupling constant,

342 closer to that in vitreous silicon [52]. These findings highlight the reorganization of the polymerized

343 silicate network (Q^4).

344   The behavior of Pb is closely related to the structural configuration it adopts, as much in the

345 pristine glass as in the alteration layer. Homogeneously dispersed within the silicate network, the

346 leaching of Pb is less favorable, and its release into solution is lower than the alkalis. When present at

347 higher concentration than in the glass studied here, Pb may form clusters, and its leaching increases,

348 probably as soon as it forms Pb-O-Pb bonds. For 45 wt% of PbO in a glass containing Na and K, it

349 has been reported that the alkalis and the lead were released at the same rate [11]. At higher

350 concentration, there is a percolation of the Pb sub-network, which is preferentially highly released into

351 solution. These high Pb contents seem to give rise to a surface enrichment in Pb [11, 12]. No such

352 enrichment was observed for our 28 wt% PbO glass; conversely, Pb is depleted in the outermost part

353 of the alteration layer. In the remaining part, it stays surrounded by Si in a stable structural

354 configuration similar to that of the pristine glass.

355   The data obtained from this work could enable parameters to be set for a simple predictive

356 mechanistic model for lead leaching from commercial lead crystal glass.

357

358

359

360

361

362

363

364

365

366

367

368

369

370

371

372 **REFERENCES**

373

374 1.   Szaloki, I.; Braun, M.; Van Grieken, R., Quantitative characterisation of the leaching of lead
375 and other elements from glazed surfaces of historical ceramics. *J. Anal. At. Spectrom.* **2000,** *15*, (7),
376 843-850.

377 2.   Cohen, B. M.; Uhlmann, D. R.; Shaw, R. R., Optical and electrical properties of lead silicate
378 glasses. *Journal of Non-Crystalline Solids* **1973,** *12*, (2), 177-188.

379 3.   Barker, R. S.; McConkey, E. A.; Richards.Da, EFFECT OF GAMMA RADIATION ON
380 OPTICAL ABSORPTION OF LEAD SILICATE GLASS. *Phys. Chem. Glasses* **1965,** *6*, (1), 24-&.

381 4.   Patrick, L., Lead toxicity, a review of the literature. Part 1: Exposure, evaluation, and
382 treatment. *Altern. Med. Rev.* **2006,** *11*, (1), 2-22.

383 5.   Graziano, J. H.; Blum, C. B.; Lolacono, N. J.; Slavkovich, V.; Manton, W. I.; Pond, S.; Moore,
384 M. R., Human in vivo model for the determination of lead bioavailability using stable isotope dilution.
385 *Environ. Health Perspect.* **1996,** *104*, (2), 176-179.

386 6.   van Elteren, J. T.; Grilc, M.; Beeston, M. P.; Reig, M. S.; Grgic, I., An integrated experimental-
387 modeling approach to study the acid leaching behavior of lead from sub-micrometer lead silicate glass
388 particles. *J. Hazard. Mater.* **2013,** *262*, 240-249.

389 7.   Rahimi, R. A.; Sadrnezhaad, S. K., Effects of Ion-Exchange and Hydrolysis Mechanisms on
390 Lead Silicate Glass Corrosion. *Corrosion* **2012,** *68*, (9), 793-800.

391 8.   Rahimi, R. A.; Sadrnezhaad, S. K.; Raisali, G.; Hamidi, A., Hydrolysis kinetics of lead silicate
392 glass in acid solution. *Journal of Nuclear Materials* **2009,** *389*, (3), 427-431.

393 9.   Sadrnezhaad, S. K.; Rahimi, R. A.; Raisali, G.; Foruzanfar, F., Mechanism of deleading of
394 silicate glass by 0.5 N HNO3. *Journal of Non-Crystalline Solids* **2009,** *355*, (48-49), 2400-2404.

395 10.   Mizuno, M.; Takahashi, M.; Takaishi, T.; Yoko, T., Leaching of lead and connectivity of
396 plumbate networks in lead silicate glasses. *J. Am. Ceram. Soc.* **2005,** *88*, (10), 2908-2912.

397 11.   Bertoncello, R.; Milanese, L.; Bouquillon, A.; Dran, J. C.; Mille, B.; Salomon, J., Leaching of
398 lead silicate glasses in acid environment: compositional and structural changes. *Appl. Phys. A-Mater.*
399 *Sci. Process.* **2004,** *79*, (2), 193-198.

400 12.   Bonnet, C.; Bouquillon, A.; Turrell, S.; Deram, V.; Mille, B.; Salomon, J.; Thomassin, J. H.;
401 Fiaud, C., Alteration of lead silicate glasses due to leaching in heated acid solutions. *Journal of Non-*
402 *Crystalline Solids* **2003,** *323*, (1-3), 214-220.

403 13.   Guadagnino, E.; Gambaro, M.; Gramiccioni, L.; Denaro, M.; Feliciani, R.; Baldin, M.; Stacchini,
404 P.; Giovannangeli, S.; Carelli, G.; Castellino, N.; Vinci, F., Estimation of lead intake from crystalware
405 under conditions of consumer use. *Food Addit. Contam.* **2000,** *17*, (3), 205-218.

406 14.   Guadagnino, E.; Verita, M.; Geotti-Bianchini, F.; Shallenberger, J.; Pantano, C. G., Surface
407 analysis of 24% lead crystal glass articles: correlation with lead release. *Glass Technol.* **2002,** *43*, (2),
408 63-69.

409 15.   Schultz-Munzenberg, C.; Meisel, W.; Gutlich, P., Changes of lead silicate glasses induced by
410 leaching. *Journal of Non-Crystalline Solids* **1998,** *238*, (1-2), 83-90.

411 16. Ahmed, A. A.; Youssof, I. M., Effect of repeated leaching on the release of lead and other
412 cations from lead crystal glass (24% PbO) by acid solutions and water. *Glass Technol.* **1997,** *38*, (5),
413 171-178.

414 17. Ahmed, A. A.; Youssof, I. M., Interaction between lead crystal glass (24 % PbO) and acetic
415 acid. *Glastech. Ber.-Glass Sci. Technol.* **1997,** *70*, (6), 173-185.

416 18. Ahmed, A. A.; Youssof, I. M., Reactions between water and lead crystal glass (24% PbO).
417 *Glass Technol.* **1997,** *38*, (1), 30-38.

418 19. Cailleteau, C.; Weigel, C.; Ledieu, A.; Barboux, P.; Devreux, F., On the effect of glass
419 composition in the dissolution of glasses by water. *Journal of Non-Crystalline Solids* **2008,** *354*, (2-9),
420 117-123.

421 20. Graziano, J. H.; Blum, C., LEAD-EXPOSURE FROM LEAD CRYSTAL. *Lancet* **1991,** *337*,
422 (8734), 141-142.

423 21. Kanunnikova, O. M.; Goncharov, O. Y., X-ray photoelectron analysis of lead-silicate glass
424 structure. *J. Appl. Spectrosc.* **2009,** *76*, (2), 194-202.

425 22. Wang, P. W.; Zhang, L. P., Structural role of lead in lead silicate glasses derived from XPS
426 spectra. *Journal of Non-Crystalline Solids* **1996,** *194*, (1-2), 129-134.

427 23. Alderman, O. L. G.; Hannon, A. C.; Holland, D.; Feller, S.; Lehr, G.; Vitale, A. J.; Hoppe, U.;
428 von Zimmerman, M.; Watenphul, A., Lone-pair distribution and plumbite network formation in high lead
429 silicate glass, 80PbO center dot 20SiO(2). *Phys. Chem. Chem. Phys.* **2013,** *15*, (22), 8506-8519.

430 24. Takaishi, T.; Takahashi, M.; Jin, J.; Uchino, T.; Yoko, T.; Takahashi, M., Structural study on
431 PbO-SiO2 glasses by X-ray and neutron diffraction and Si-29 MAS NMR measurements. *J. Am.*
432 *Ceram. Soc.* **2005,** *88*, (6), 1591-1596.

433 25. Gee, I. A.; Holland, D.; McConville, C. F., Atomic environments in binary lead silicate and
434 ternary alkali lead silicate glasses. *Phys. Chem. Glasses* **2001,** *42*, (6), 339-348.

435 26. Fayon, F.; Landron, C.; Sakurai, K.; Bessada, C.; Massiot, D., Pb2+ environment in lead
436 silicate glasses probed by Pb-L-III edge XAFS and Pb-207 NMR. *Journal of Non-Crystalline Solids*
437 **1999,** *243*, (1), 39-44.

438 27. Feller, S.; Lodden, G.; Riley, A.; Edwards, T.; Croskrey, J.; Schue, A.; Liss, D.; Stentz, D.;
439 Blair, S.; Kelley, M.; Smith, G.; Singleton, S.; Affatigato, M.; Holland, D.; Smith, M. E.; Kamitsos, E. I.;
440 Varsamis, C. P. E.; Ioannou, E., A multispectroscopic structural study of lead silicate glasses over an
441 extended range of compositions. *Journal of Non-Crystalline Solids* **2010,** *356*, (6-8), 304-313.

442 28. Fajans, K.; Kreidl, N. J., STABILITY OF LEAD GLASSES AND POLARIZATION OF IONS. *J.*
443 *Am. Ceram. Soc.* **1948,** *31*, (4), 105-114.

444 29. Carmona, N.; Garcia-Heras, M.; Gil, C.; Villegas, M. A., Chemical degradation of glasses
445 under simulated marine medium. *Mater. Chem. Phys.* **2005,** *94*, (1), 92-102.

446 30. Hight, S. C., Lead migration from lead crystal wine glasses. *Food Addit. Contam.* **1996,** *13*,
447 (7), 747-765.

448 31. Angeli, F.; Charpentier, T.; Gaillard, M.; Jollivet, P., Influence of zirconium on the structure of
449 pristine and leached soda-lime borosilicate glasses: Towards a quantitative approach by O-17
450 MQMAS NMR. *Journal of Non-Crystalline Solids* **2008,** *354*, (31), 3713-3722.

451 32.   Larsen, F. H.; Farnan, I., Si-29 and O-17 (Q)CPMG-MAS solid-state NMR experiments as an
452 optimum approach for half-integer nuclei having long T-1 relaxation times. *Chem. Phys. Lett.* **2002,**
453 *357*, (5-6), 403-408.

454 33.   Amoureux, J. P.; Fernandez, C.; Steuernagel, S., Z filtering in MQMAS NMR. *J. Magn. Reson.*
455 *Ser. A* **1996,** *123*, (1), 116-118.

456 34.   Fernandez, C.; Amoureux, J. P., 2D MULTIQUANTUM MAS-NMR SPECTROSCOPY OF AL-
457 27 IN ALUMINOPHOSPHATE MOLECULAR-SIEVES. *Chem. Phys. Lett.* **1995,** *242*, (4-5), 449-454.

458 35.   Angeli, F.; Villain, O.; Schuller, S.; Ispas, S.; Charpentier, T., Insight into sodium silicate glass
459 structural organization by multinuclear NMR combined with first-principles calculations. *Geochim.*
460 *Cosmochim. Acta* **2011,** *75*, (9), 2453-2469.

461 36.   Fayon, F.; Bessada, C.; Massiot, D.; Farnan, I.; Coutures, J. P., Si-29 and Pb-207 NMR study
462 of local order in lead silicate glasses. *Journal of Non-Crystalline Solids* **1998,** *232*, 403-408.

463 37.   Shrikhande, V. K.; Sudarsan, V.; Kothiyal, G. P.; Kulshreshtha, S. K., Si-29 MAS NMR and
464 microhardness studies of some lead silicate glasses with and without modifiers. *Journal of Non-*
465 *Crystalline Solids* **2001,** *283*, (1-3), 18-26.

466 38.   Lee, S. K.; Kim, E. J., Probing Metal-Bridging Oxygen and Configurational Disorder in
467 Amorphous Lead Silicates: Insights from O-17 Solid-State Nuclear Magnetic Resonance. *Journal of*
468 *Physical Chemistry C* **2015,** *119*, (1), 748-756.

469 39.   Florian, P.; Vermillion, K. E.; Grandinetti, P. J.; Farnan, I.; Stebbins, J. F., Cation distribution in
470 mixed alkali disilicate glasses. *J. Am. Chem. Soc.* **1996,** *118*, (14), 3493-3497.

471 40.   Lee, S. K.; Stebbins, J. F., Effects of the degree of polymerization on the structure of sodium
472 silicate and aluminosilicate glasses and melts: An O-17 NMR study. *Geochim. Cosmochim. Acta* **2009,**
473 *73*, (4), 1109-1119.

474 41.   Clark, T. M.; Grandinetti, P. J., Calculation of bridging oxygen O-17 quadrupolar coupling
475 parameters in alkali silicates: A combined ab initio investigation. *Solid State Nucl. Magn. Reson.* **2005,**
476 *27*, (4), 233-241.

477 42.   Clark, T. M.; Grandinetti, P. J.; Florian, P.; Stebbins, J. F., An O-17 NMR investigation of
478 crystalline sodium metasilicate: Implications for the determination of local structure in alkali silicates.
479 *Journal of Physical Chemistry B* **2001,** *105*, (49), 12257-12265.

480 43.   Ashbrook, S. E.; Berry, A. J.; Wimperis, S., O-17 multiple-quantum MAS NMR study of high-
481 pressure hydrous magnesium silicates. *J. Am. Chem. Soc.* **2001,** *123*, (26), 6360-6366.

482 44.   Ashbrook, S. E.; Berry, A. J.; Wimperis, S., O-17 multiple-quantum MAS NMR study of
483 pyroxenes. *Journal of Physical Chemistry B* **2002,** *106*, (4), 773-778.

484 45.   Lee, S. K.; Stebbins, J. F., Nature of cation mixing and ordering in Na-Ca silicate glasses and
485 melts. *Journal of Physical Chemistry B* **2003,** *107*, (14), 3141-3148.

486 46.   Angeli, F.; Charpentier, T.; Molieres, E.; Soleilhavoup, A.; Jollivet, P.; Gin, S., Influence of
487 lanthanum on borosilicate glass structure: A multinuclear MAS and MQMAS NMR investigation.
488 *Journal of Non-Crystalline Solids* **2013,** *376*, 189-198.

489 47.   Gin, S.; Jollivet, P.; Fournier, M.; Angeli, F.; Frugier, P.; Charpentier, T., Origin and
490 consequences of silicate glass passivation by surface layers. *Nature Communications* **2015,** *6*.

491   48.   Helebrant, A.; Pekarkova, I., Kinetics of glass corrosion in acid solutions. *Ber. Bunsen-Ges.*
492   *Phys. Chem. Chem. Phys.* **1996,** *100*, (9), 1519-1522.
493   49.   Apelblat, A.; Manzurola, E., Solubilities of manganese, cadmium, mercury and lead acetates in
494   water from T=278.15 K to T=340.15 K. *J. Chem. Thermodyn.* **2001,** *33*, (2), 147-153.
495   50.   Fournier, M.; Ull, A.; Nicoleau, E.; Inagaki, Y.; Odorico, M.; Frugier, P.; Gin, S., Glass
496   dissolution rate measurement and calculation revisited. *Journal of Nuclear Materials* **2016,** *476*, 140-
497   154.
498   51.   Brunet, F.; Charpentier, T.; Le Caer, S.; Renault, J. P., Solid-state NMR characterization of a
499   controlled-pore glass and of the effects of electron irradiation. *Solid State Nucl. Magn. Reson.* **2008,**
500   *33*, (1-2), 1-11.
501   52.   Charpentier, T.; Kroll, P.; Mauri, F., First-Principles Nuclear Magnetic Resonance Structural
502   Analysis of Vitreous Silica. *Journal of Physical Chemistry C* **2009,** *113*, (18), 7917-7929.

503

504

505

506

507

508

509

510

511

512

513

514

515

516

517

518

519

520

521

522

523

524

525

526

Table caption

528

	Site	¹⁷O NMR Parameters		Proportion from composition	Proportion from ¹⁷O NMR
Pristine glass	**Si-O-Si**		52.5 (7.3)	78 %	78 %
		$C_Q(MHz) - (\sigma_{C_Q})$	4.8 (0.3)		
		$\eta_Q - (\sigma_{\eta_Q})$	0.3 (0.1)		
	Si-O-(Pb,K)	$\delta_{iso}(ppm) - (\sigma_{\delta_{iso}})$	118.7 (10.8)	9 % (Si-O-Pb)	14 %
		$C_Q(MHz) - (\sigma_{C_Q})$	3.1 (0.5)		
		$\eta_Q - (\sigma_{\eta_Q})$	0.6 (0.2)		
	Si-O-K	$\delta_{iso}(ppm) - (\sigma_{\delta_{iso}})$	74.8 (9.2)	13 %	8 %
		$C_Q(MHz) - (\sigma_{C_Q})$	2.2 (0.5)		
		$\eta_Q - (\sigma_{\eta_Q})$	0.6 (0.2)		
Altered glass	**Si-O-Si**	$\delta_{iso}(ppm) - (\sigma_{\delta_{iso}})$	42.0 (5.0)	89 %	89 %
		$C_Q(MHz) - (\sigma_{C_Q})$	5.2 (0.2)		
		$\eta_Q - (\sigma_{\eta_Q})$	0.2 (0.1)		
	Si-O-(Pb,K)	$\delta_{iso}(ppm) - (\sigma_{\delta_{iso}})$	130.0 (12.0)	8 % (Si-O-Pb)	6 %
		$C_Q(MHz) - (\sigma_{C_Q})$	3.1 (0.5)		
		$\eta_Q - (\sigma_{\eta_Q})$	0.6 (0.2)		
	Si-O-K	$\delta_{iso}(ppm) - (\sigma_{\delta_{iso}})$	74.8 (9.2)	3 %	1 %
		$C_Q(MHz) - (\sigma_{C_Q})$	2.2 (0.5)		
		$\eta_Q - (\sigma_{\eta_Q})$	0.6 (0.2)		
	Si-O-H	$\delta_{iso}(ppm) - (\sigma_{\delta_{iso}})$	130.0 (12.0)	-	4 %
		$C_Q(MHz) - (\sigma_{C_Q})$	3.1 (0.5)		
		$\eta_Q - (\sigma_{\eta_Q})$	0.6 (0.2)		

529

530 **Table 1.** ¹⁷O NMR parameters obtained by fitting the ¹⁷O MAS NMR data of pristine and altered glass
531 *(standard deviations, depending on the distribution of each parameter, are indicated in parentheses)*
532 *using as constraints the parameters extracted from the MQMAS data. The C_Q precision is 0.25 MHz*
533 *and δ_{iso} precision is 2 ppm. The site proportions, calculated from pristine and altered glass*
534 *compositions, and from the ¹⁷O MAS NMR data, are reported.*

535
536
537
538
539
540
541

542 **Figure caption**

543

544 *(a)*   *(b)*
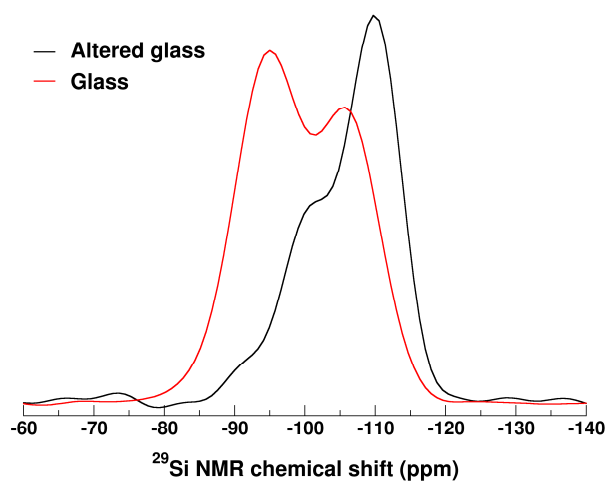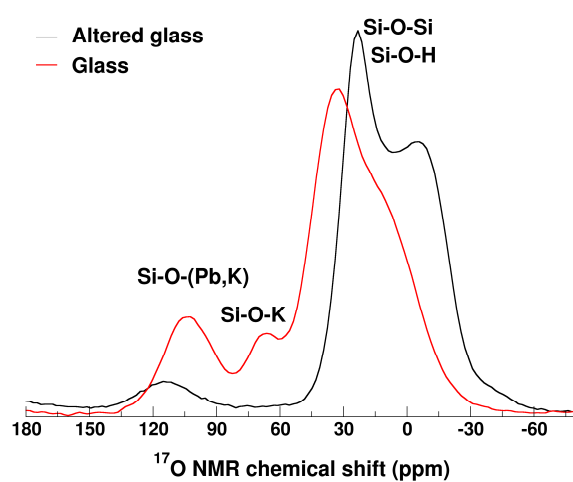
546 ***Figure 1.*** *(a) ^{29}Si MAS NMR and (b) ^{17}O MAS NMR spectra of pristine and altered glass after 35 days*

547 *at 70℃ in acetic acid solution with oxygen-17 enri ched water.*

548

549

550

551

552

553

554
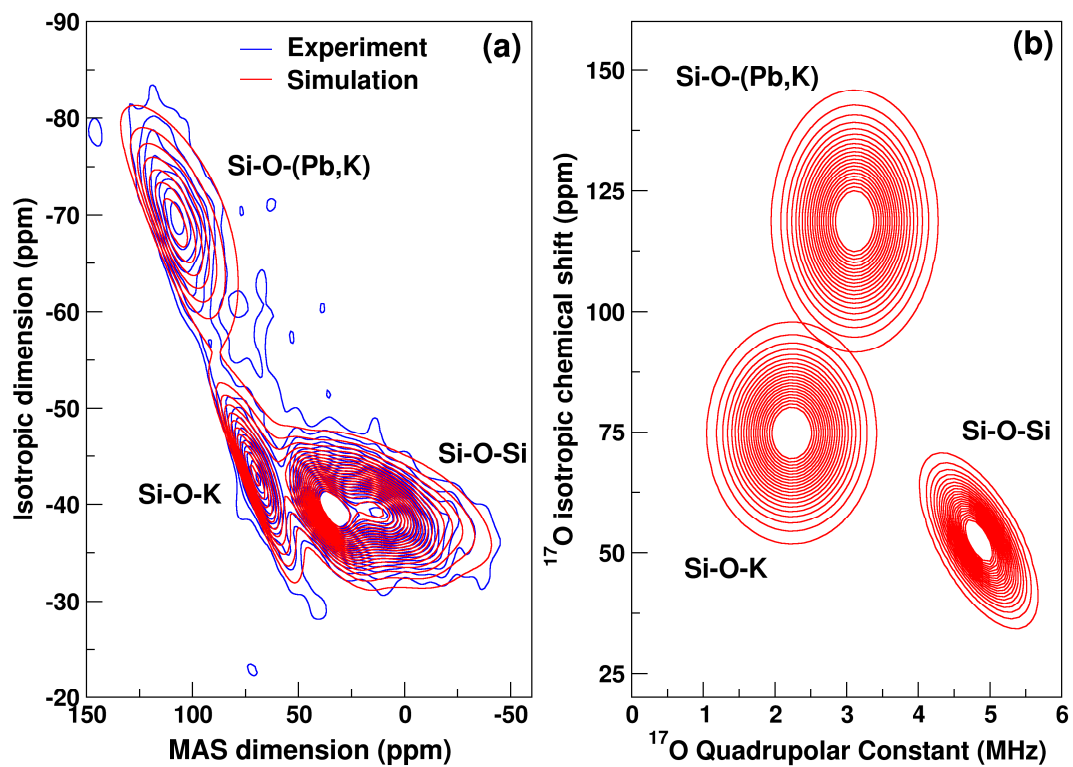
Figure 2. *(a) Contour plots of the experimental and simulated ^{17}O MQMAS spectra and (b) the two-dimensional projection of the extracted ^{17}O NMR parameter distributions δ_{iso} and C_Q.*

576 *(a)*

577

578 *(c)*
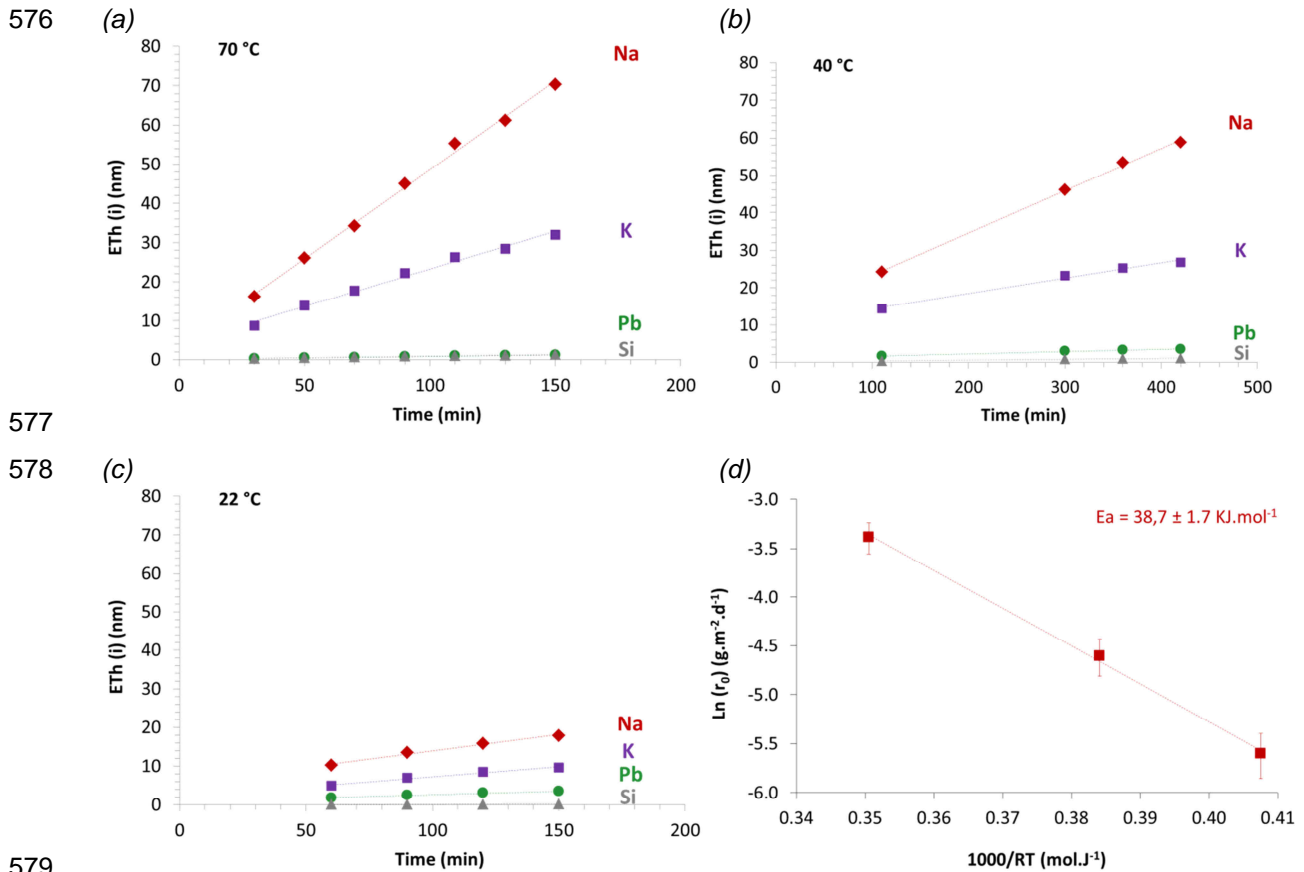
579

580 **Figure 3**. *Equivalent thickness of altered glass calculated from the release of Si at 22°C (a), 40°C (b)*

581 *and 70°C (c) in acetic acid, in forward dissolution rate regime. (d) Determination of the apparent*

582 *activation energy for the alteration mechanisms in forward dissolution rate regime. Broken lines are*

583 *simple visual aids.*

584

585

586

587

588

589

590

591

592

593

594

595

596

597

19

598

599 *(a)*

(b)

600

601 *(c)*

(d)
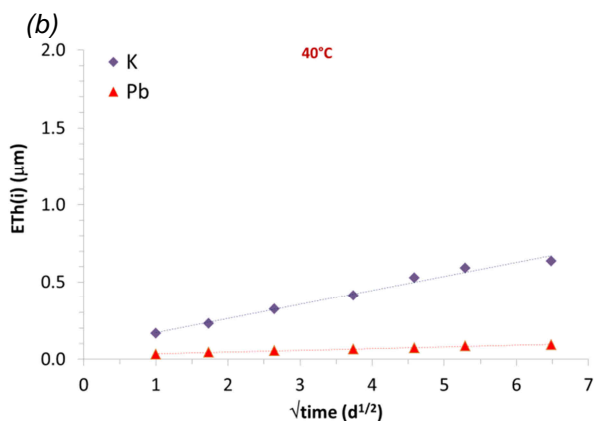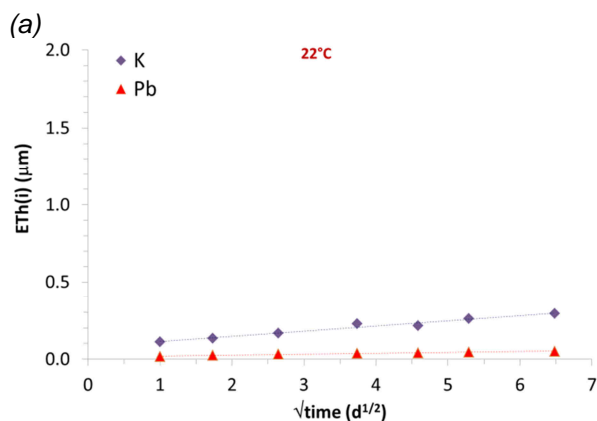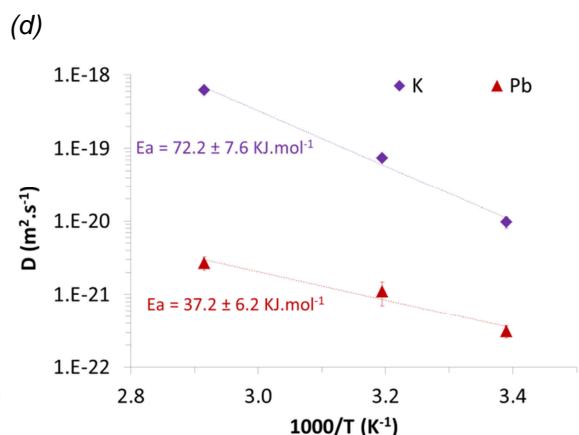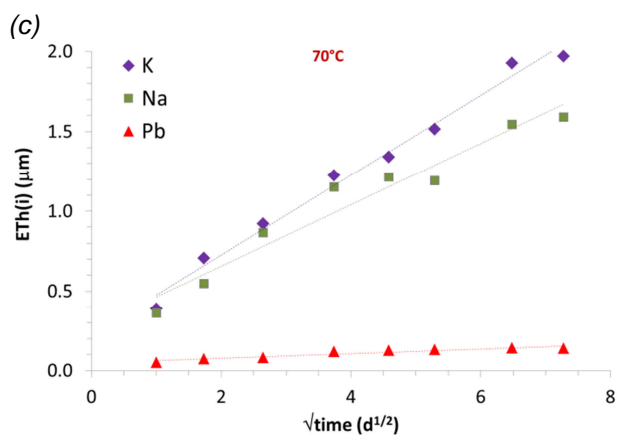
602

603

604 **Figure 4**. *Equivalent thickness of altered glass calculated from the leaching of Pb and of K at 22°C*

605 *(a), 40°C (b) and 70°C (b) in acetic acid solution,   in a solution initially saturated with respect to*

606 *amorphous silica. (d) Representation of the diffusion coefficients depending on the temperature. The*

607 *activation energy (Ea) is given by the slope of the line. Broken lines are simple visual aids.*

608

609

610

611

612

613

614

615

616

617

618

619

620

621

622 *(a)* *(b)*

623
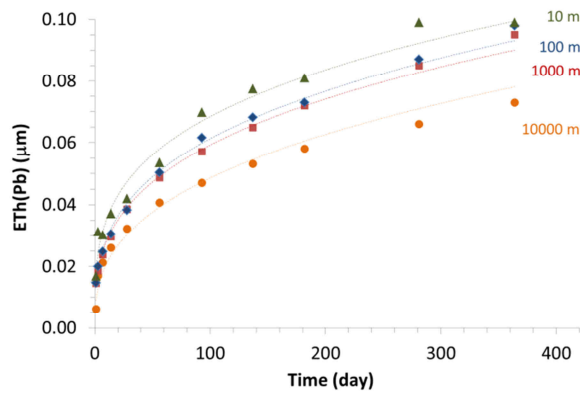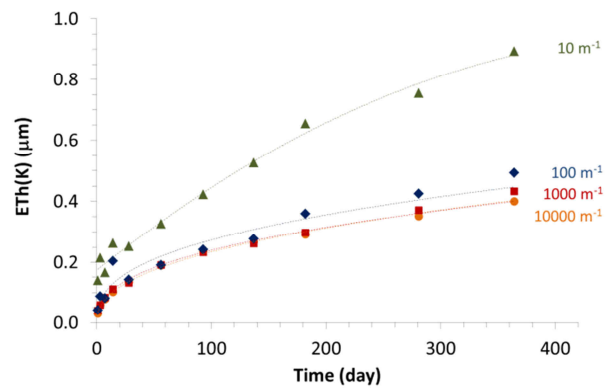
624

625

626 **Figure 5**. *Equivalent thickness of altered glass calculated from the release of (a) Pb and (b) K at 22°C*

627 *in acetic acid solution for different SA/V ratios (10, 100, 1000 and 10000 m⁻¹). Broken lines are simple*

628 *visual aids.*

629
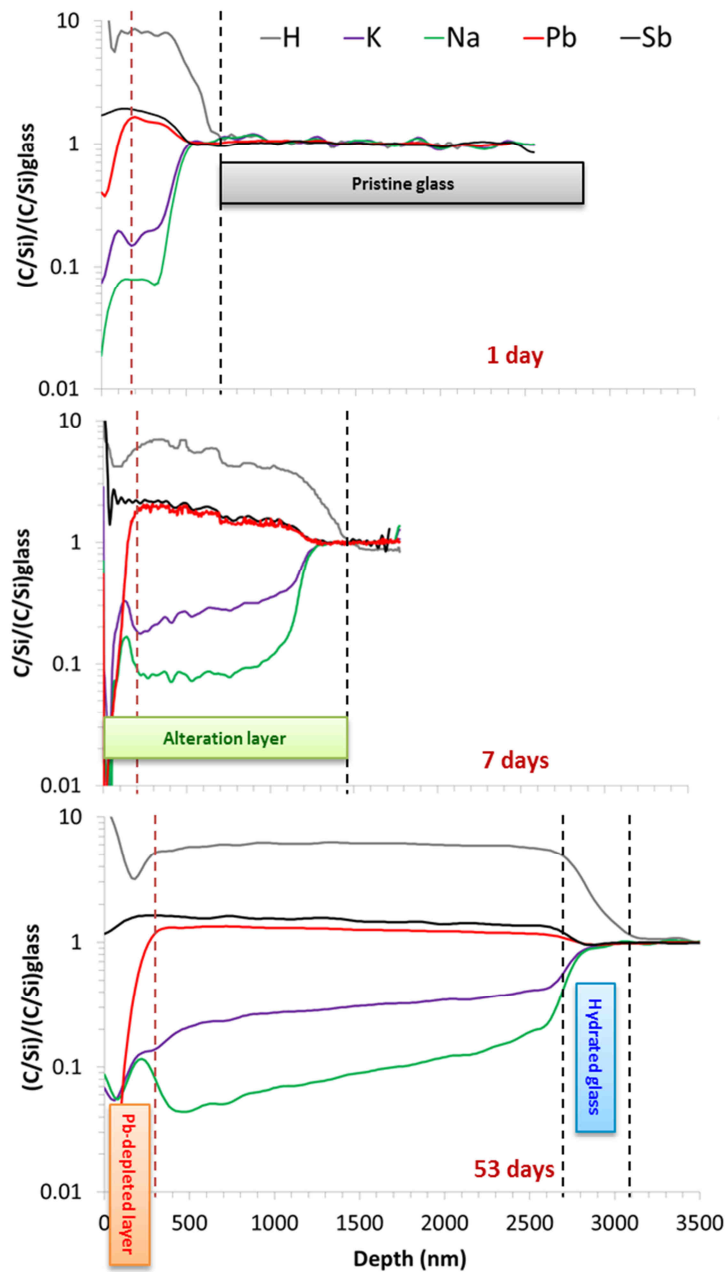
Figure 6. *Elemental profiles obtained by ToF-SIMS on the glass altered at 70℃ for 1, 7 and 53 days in acetic acid solution saturated with respect to amorphous silica. Data have been normalized compared to Si, which is the least soluble element. All the elements are thus normalized to 1 in the pristine glass; data lower than 1 indicate a depletion of the element, whereas data higher than 1 indicate an enrichment*
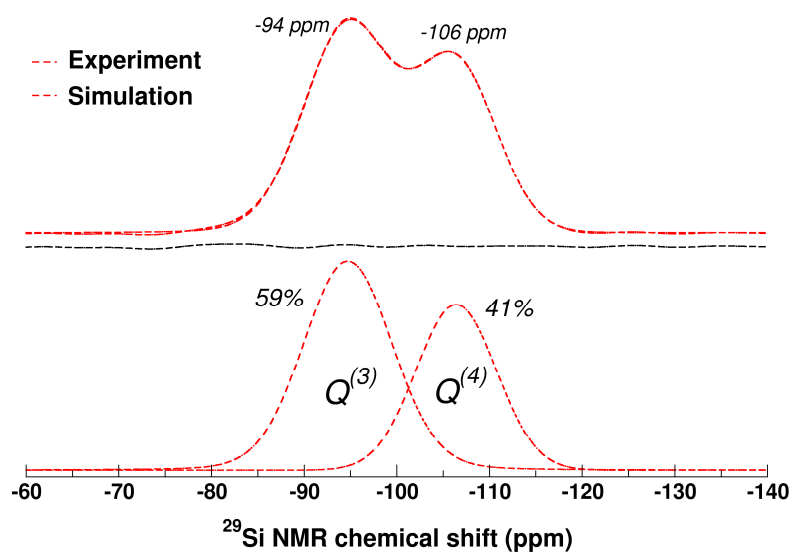
Figure S1. ^{29}Si MAS NMR spectra of pristine glass (solid line) and simulated spectra (dotted lines)
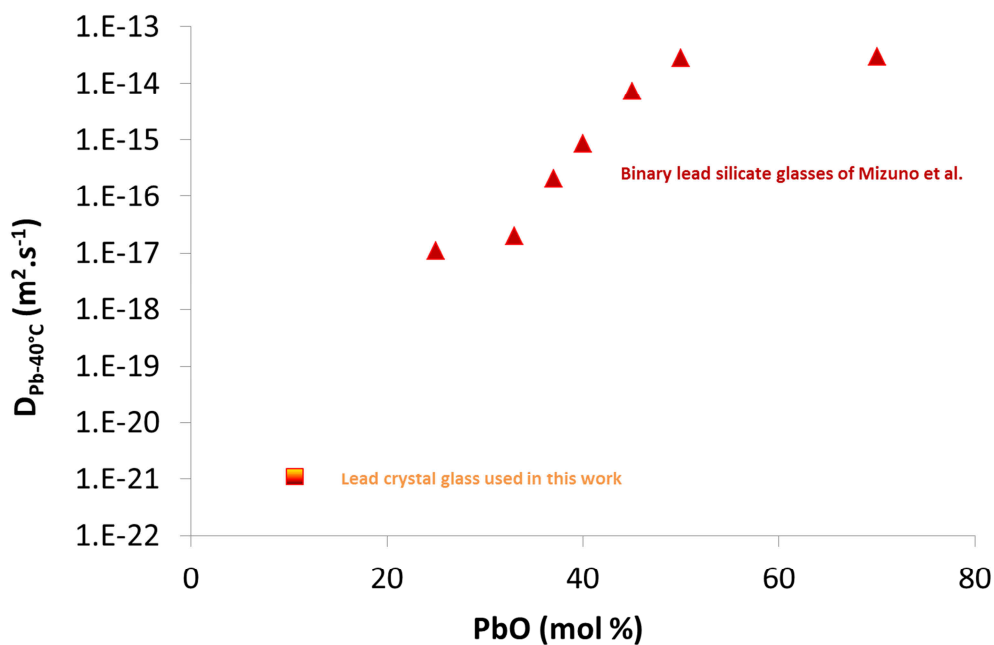
Figure S2. Comparison of diffusion coefficients measured at 40℃ in the lead crystal glass used in this work and in binary lead silicate glasses of Mizuno et al. [10].

655   (a)

656
657   (b)
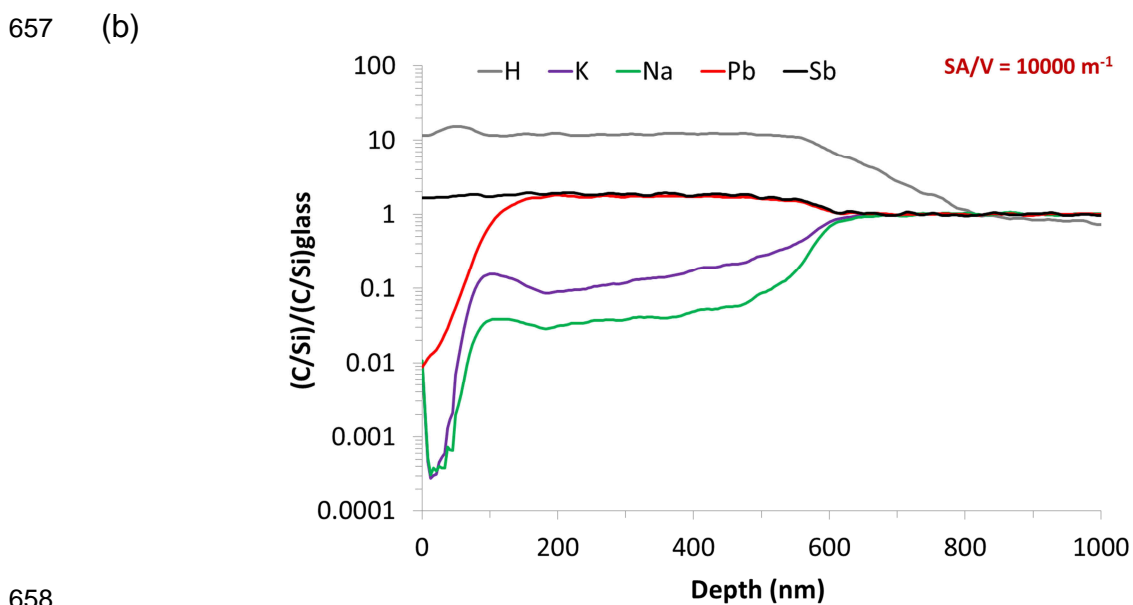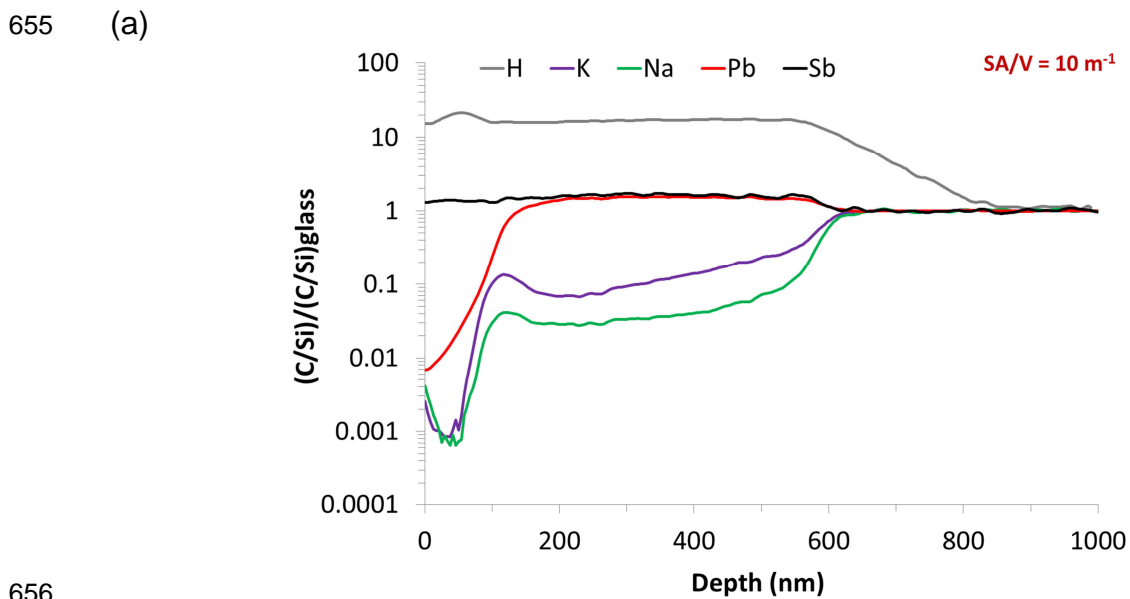
658
659
660   **Figure S3.** *Elemental profiles obtained by ToF-SIMS on the glass altered at 22°C for 1 year in acetic*
661   *acid solution with SA/V = 10 m⁻¹ (a) and SA/V = 10000 m⁻¹ (b). Data have been normalized compared*
662   *to Si, which is the least soluble element. All the elements are thus normalized to 1 in the pristine glass;*
663   *data lower than 1 indicate a depletion of the element, whereas data higher than 1 indicate an*
664   *enrichment.*
665
666
667
668
669
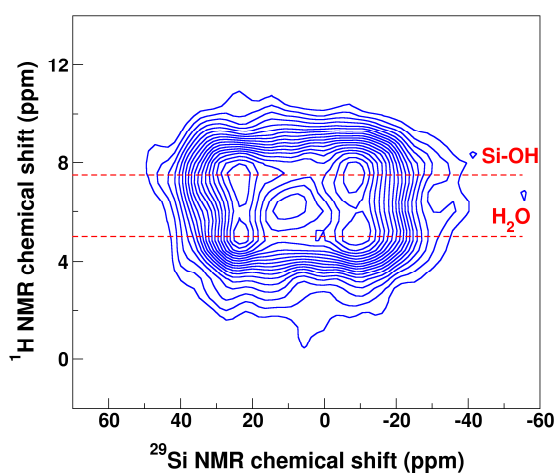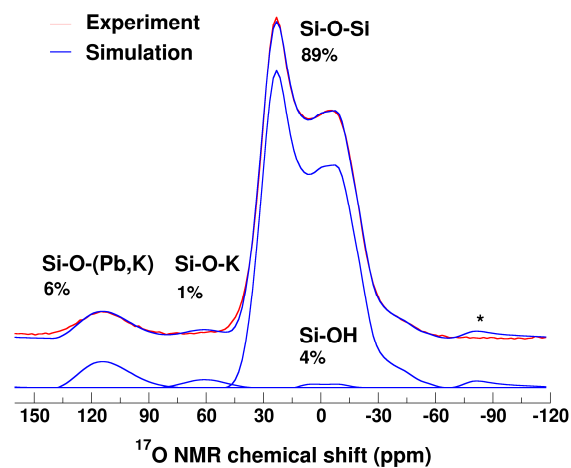
Figure S4. *(a) $^1H \rightarrow ^{17}O$ HETCOR spectra with 2 ms polarization time of altered glass.*

(b) Simulation of the ^{17}O MAS NMR spectra of altered glass

(35 days at 70℃ in acetic acid solution with oxyge n-17 enriched water).

696
697 For Table of Contents Only
698
699

26